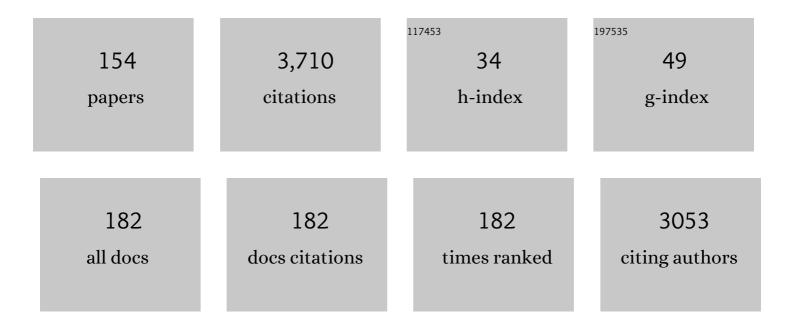
Sandra C Piazolo

List of Publications by Year in descending order

Source: https://exaly.com/author-pdf/1304200/publications.pdf Version: 2024-02-01



#	Article	IF	CITATIONS
1	Deformation-induced trace element redistribution in zircon revealed using atom probe tomography. Nature Communications, 2016, 7, 10490.	5.8	137
2	Tectonic significance of deformation patterns in granitoid rocks of the Menderes nappes, Anatolide belt, southwest Turkey. International Journal of Earth Sciences, 2001, 89, 766-780.	0.9	115
3	The weighted Burgers vector: a new quantity for constraining dislocation densities and types using electron backscatter diffraction on 2D sections through crystalline materials. Journal of Microscopy, 2009, 233, 482-494.	0.8	85
4	Controls on lineation development in low to medium grade shear zones: a study from the Cap de Creus peninsula, NE Spain. Journal of Structural Geology, 2002, 24, 25-44.	1.0	78
5	The initiation of strain localisation in plagioclase-rich rocks: Insights from detailed microstructural analyses. Journal of Structural Geology, 2010, 32, 1404-1416.	1.0	78
6	Evaluating quartz crystallographic preferred orientations and the role of deformation partitioning using EBSD and fabric analyser techniques. Journal of Structural Geology, 2010, 32, 803-817.	1.0	75
7	Brittle-ductile microfabrics in naturally deformed zircon: Deformation mechanisms and consequences for U-Pb dating. American Mineralogist, 2012, 97, 1544-1563.	0.9	73
8	Halogen-bearing minerals in syenites and high-grade marbles of Dronning Maud Land, Antarctica: monitors of fluid compositional changes during late-magmatic fluid-rock interaction processes. Contributions To Mineralogy and Petrology, 1998, 132, 246-268.	1.2	72
9	Temperature dependent grain boundary migration in deformed-then-annealed material: Observations from experimentally deformed synthetic rocksalt. Tectonophysics, 2006, 427, 55-71.	0.9	70
10	The effect of Dauphiné twinning on plastic strain in quartz. Contributions To Mineralogy and Petrology, 2011, 161, 635-652.	1.2	66
11	Making EBSD on water ice routine. Journal of Microscopy, 2015, 259, 237-256.	0.8	64
12	Are polymers suitable rock analogs?. Tectonophysics, 2002, 350, 35-47.	0.9	63
13	Microstructural evolution during initial stages of static recovery and recrystallization: new insights from in-situ heating experiments combined with electron backscatter diffraction analysis. Journal of Structural Geology, 2005, 27, 447-457.	1.0	63
14	Effect of surface orientation on dissolution rates and topography of CaF2. Geochimica Et Cosmochimica Acta, 2012, 86, 392-403.	1.6	62
15	Stability of high-Al titanite from low-pressure calcsilicates in light of fluid and host-rock composition. American Mineralogist, 1999, 84, 37-47.	0.9	59
16	Stylolite interfaces and surrounding matrix material: Nature and role of heterogeneities in roughness and microstructural development. Journal of Structural Geology, 2010, 32, 1070-1084.	1.0	55
17	Microstructure and fabric development in ice: Lessons learned from in situ experiments and implications for understanding rock evolution. Journal of Structural Geology, 2014, 61, 50-77.	1.0	55
18	Subâ€structure characterization of experimentally and naturally deformed ice using cryoâ€EBSD. Journal of Microscopy, 2008, 230, 509-519.	0.8	54

#	Article	IF	CITATIONS
19	The geodynamic evolution of Mesoarchean anorthosite complexes inferred from the Naajat Kuuat Complex, southern West Greenland. Precambrian Research, 2012, 196-197, 149-170.	1.2	53
20	Brittle fracturing and fracture healing of zircon: An integrated cathodoluminescence, EBSD, U-Th-Pb, and REE study. American Mineralogist, 2007, 92, 1213-1224.	0.9	46
21	Structure of grain boundaries in wet, synthetic polycrystalline, statically recrystallizing halite - evidence from cryo-SEM observations. Geofluids, 2006, 6, 93-104.	0.3	45
22	Chemical and physical heterogeneity within native gold: implications for the design of gold particle studies. Mineralium Deposita, 2021, 56, 1563-1588.	1.7	44
23	Measurements and full-field predictions of deformation heterogeneities in ice. Earth and Planetary Science Letters, 2011, 305, 153-160.	1.8	43
24	Messengers from the deep: Fossil wadsleyite-chromite microstructures from the Mantle Transition Zone. Scientific Reports, 2015, 5, 16484.	1.6	43
25	A new type of numerical experiment on the spatial and temporal patterns of localization of deformation in a material with a coupling of grain size and rheology. Earth and Planetary Science Letters, 2005, 239, 309-326.	1.8	40
26	Process of magnetite fabric development during granite deformation. Earth and Planetary Science Letters, 2011, 308, 77-89.	1.8	39
27	Hydrothermal replacement of Aragonite by Calcite: interplay between replacement, fracturing and growth. European Journal of Mineralogy, 2013, 25, 123-136.	0.4	39
28	Atomic worlds: Current state and future of atom probe tomography in geoscience. Scripta Materialia, 2018, 148, 115-121.	2.6	39
29	Hornblendite delineates zones of mass transfer through the lower crust. Scientific Reports, 2016, 6, 31369.	1.6	38
30	Humite- and scapolite-bearing assemblages in marbles and calcsilicates of Dronning Maud Land, Antarctica: new data for Gondwana reconstructions. Journal of Metamorphic Geology, 1999, 17, 91-107.	1.6	36
31	A spectroscopic and carbon-isotope study of mixed-habit diamonds: Impurity characteristics and growth environment. American Mineralogist, 2013, 98, 66-77.	0.9	36
32	Local partial melting of the lower crust triggered by hydration through melt–rock interaction: an example from Fiordland, New Zealand. Journal of Metamorphic Geology, 2017, 35, 213-230.	1.6	36
33	Tectonic cycles of the New England Orogen, eastern Australia: A Review. Australian Journal of Earth Sciences, 2019, 66, 459-496.	0.4	36
34	Lightning strikes as a major facilitator of prebiotic phosphorus reduction on early Earth. Nature Communications, 2021, 12, 1535.	5.8	36
35	The influence of matrix rheology and vorticity on fabric development of populations of rigid objects during plane strain deformation. Tectonophysics, 2002, 351, 315-329.	0.9	35
36	Deformation-resembling microstructure created by fluid-mediated dissolution–precipitation reactions. Nature Communications, 2017, 8, 14032.	5.8	34

#	Article	IF	CITATIONS
37	Brittle-plastic deformation in initially dry rocks at fluid-present conditions: transient behaviour of feldspar at mid-crustal levels. Contributions To Mineralogy and Petrology, 2012, 163, 403-425.	1.2	33
38	The influence of phase and grain size distribution on the dynamics of strain localization in polymineralic rocks. Journal of Structural Geology, 2015, 72, 15-32.	1.0	33
39	The use of combined cathodoluminescence and EBSD analysis: a case study investigating grain boundary migration mechanisms in quartz. Journal of Microscopy, 2005, 217, 152-161.	0.8	32
40	Numerical simulations of microstructures using the Elle platform: A modern research and teaching tool. Journal of the Geological Society of India, 2010, 75, 110-127.	0.5	32
41	Mass transfer in the lower crust: Evidence for incipient melt assisted flow along grain boundaries in the deep arc granulites of Fiordland, New Zealand. Geochemistry, Geophysics, Geosystems, 2016, 17, 3733-3753.	1.0	32
42	Redox-freezing and nucleation of diamond via magnetite formation in the Earth's mantle. Nature Communications, 2016, 7, 11891.	5.8	31
43	Fluid-present deformation aids chemical modification of chromite: Insights from chromites from Golyamo Kamenyane, SE Bulgaria. Lithos, 2015, 228-229, 78-89.	0.6	30
44	The recognition of former melt flux through highâ€strain zones. Journal of Metamorphic Geology, 2018, 36, 1049-1069.	1.6	30
45	Dominance of microstructural processes and their effect on microstructural development: insights from numerical modelling of dynamic recrystallization. Geological Society Special Publication, 2002, 200, 149-170.	0.8	29
46	Olivine Pseudomorphs after Serpentinized Orthopyroxene Record Transient Oceanic Lithospheric Mantle Dehydration (Leka Ophiolite Complex, Norway). Journal of Petrology, 2012, 53, 1943-1968.	1.1	29
47	Quantitative characterization of plastic deformation of single diamond crystals: A high pressure high temperature (HPHT) experimental deformation study combined with electron backscatter diffraction (EBSD). Diamond and Related Materials, 2012, 30, 20-30.	1.8	29
48	The effect of preâ€ŧectonic reaction and annealing extent on behaviour during subsequent deformation: insights from paired shear zones in the lower crust of Fiordland, New Zealand. Journal of Metamorphic Geology, 2015, 33, 557-577.	1.6	29
49	Effect of local stress heterogeneities on dislocation fields: Examples from transient creep in polycrystalline ice. Acta Materialia, 2015, 90, 303-309.	3.8	29
50	The Anita Peridotite, New Zealand: Ultra-depletion and Subtle Enrichment in Sub-arc Mantle. Journal of Petrology, 2016, 57, 717-750.	1.1	28
51	Patterns of strain localization in heterogeneous, polycrystalline rocks – a numerical perspective. Earth and Planetary Science Letters, 2017, 463, 253-265.	1.8	28
52	Atom probe tomography analysis of the reference zircon gj-1: An interlaboratory study. Chemical Geology, 2018, 495, 27-35.	1.4	27
53	Quantification of the microstructural evolution of polycrystalline fabrics using FAME: Application to in situ deformation of ice. Journal of Structural Geology, 2014, 61, 109-122.	1.0	26
54	The integration of experimental in-situ EBSD observations and numerical simulations: a novel technique of microstructural process analysis. Journal of Microscopy, 2004, 213, 273-284.	0.8	25

#	Article	IF	CITATIONS
55	Dynamics of ice mass deformation: Linking processes to rheology, texture, and microstructure. Geochemistry, Geophysics, Geosystems, 2013, 14, 4185-4194.	1.0	25
56	The importance of fracture-healing on the deformation of fluid-filled layered systems. Journal of Structural Geology, 2014, 67, 94-106.	1.0	25
57	Strain localization in brittle–ductile shear zones: fluid-abundant vs. fluid-limited conditions (an) Tj ETQq1 1 0.78	84314 rgB 1.2	T /Overlock
58	Laser-Assisted Atom Probe Tomography of Deformed Minerals: A Zircon Case Study. Microscopy and Microanalysis, 2017, 23, 404-413.	0.2	25
59	Melt-present shear zones enable intracontinental orogenesis. Geology, 2020, 48, 643-648.	2.0	25
60	Pinch and swell structures: evidence for strain localisation by brittle–viscous behaviour in the middle crust. Solid Earth, 2015, 6, 1045-1061.	1.2	24
61	Trace element homogeneity from micron- to atomic scale: Implication for the suitability of the zircon GJ-1 as a trace element reference material. Chemical Geology, 2017, 456, 10-18.	1.4	24
62	Zircon Uâ€Pb Dating of a Lower Crustal Shear Zone: A Case Study From the Northern Sector of the Ivreaâ€Verbano Zone (Val Cannobina, Italy). Tectonics, 2018, 37, 322-342.	1.3	24
63	Symplectite formation in the presence of a reactive fluid: insights from hydrothermal experiments. Journal of Metamorphic Geology, 2017, 35, 281-299.	1.6	23
64	Chemical Signatures of Melt–Rock Interaction in the Root of a Magmatic Arc. Journal of Petrology, 2018, 59, 321-340.	1.1	23
65	Subgrain Rotation Recrystallization During Shearing: Insights From Fullâ€Field Numerical Simulations of Halite Polycrystals. Journal of Geophysical Research: Solid Earth, 2017, 122, 8810-8827.	1.4	22
66	Recurrent magmatic activity on a lithosphere-scale structure: Crystallization and deformation in kimberlitic zircons. Gondwana Research, 2017, 42, 126-132.	3.0	22
67	A review of numerical modelling of the dynamics of microstructural development in rocks and ice: Past, present and future. Journal of Structural Geology, 2019, 125, 111-123.	1.0	22
68	Ultrahigh temperature deformation microstructures in felsic granulites of the Napier Complex, Antarctica. Tectonophysics, 2006, 427, 133-151.	0.9	21
69	Post-deformational annealing at the subgrain scale: Temperature dependent behaviour revealed by in-situ heating experiments on deformed single crystal halite. Journal of Structural Geology, 2010, 32, 982-996.	1.0	21
70	Importance of surface structure on dissolution of fluorite: Implications for surface dynamics and dissolution rates. Geochimica Et Cosmochimica Acta, 2014, 126, 398-410.	1.6	21
71	Fabric development during exhumation from ultrahigh-pressure in an eclogite-bearing shear zone, Western Gneiss Region, Norway. Journal of Structural Geology, 2015, 71, 58-70.	1.0	21
72	The field and microstructural signatures of deformationâ€assisted melt transfer: Insights from magmatic arc lower crust, New Zealand. Journal of Metamorphic Geology, 2019, 37, 795-821.	1.6	21

#	Article	IF	CITATIONS
73	Orthopyroxene–omphacite- and garnet–omphacite-bearing magmatic assemblages, Breaksea Orthogneiss, New Zealand: Oxidation state controlled by high-P oxide fractionation. Lithos, 2015, 216-217, 1-16.	0.6	20
74	Non-basal dislocations should be accounted for in simulating ice mass flow. Earth and Planetary Science Letters, 2017, 473, 247-255.	1.8	20
75	Compositional boundary layers trigger liquid unmixing in a basaltic crystal mush. Nature Communications, 2019, 10, 4821.	5.8	20
76	Shape of pinch and swell structures as a viscosity indicator: Application to lower crustal polyphase rocks. Journal of Structural Geology, 2016, 88, 32-45.	1.0	19
77	Intracontinental Orogeny Enhanced by Farâ€Field Extension and Local Weak Crust. Tectonics, 2018, 37, 4421-4443.	1.3	19
78	Evaluating the importance of metamorphism in the foundering of continental crust. Scientific Reports, 2017, 7, 13039.	1.6	18
79	Grainâ€scale dependency of metamorphic reaction on crystal plastic strain. Journal of Metamorphic Geology, 2019, 37, 1021-1036.	1.6	17
80	Microstructurally controlled trace element (Zr, U–Pb) concentrations in metamorphic rutile: An example from the amphibolites of the Bergen Arcs. Journal of Metamorphic Geology, 2020, 38, 103-127.	1.6	17
81	Interaction of chemical and physical processes during deformation at fluid-present conditions: a case study from an anorthosite–leucogabbro deformed at amphibolite facies conditions. Contributions To Mineralogy and Petrology, 2013, 165, 543-562.	1.2	16
82	What happens to deformed rocks after deformation? A refined model for recovery based on numerical simulations. Geological Society Special Publication, 2014, 394, 215-234.	0.8	16
83	Seismic anisotropy from compositional banding in granulites from the deep magmatic arc of Fiordland, New Zealand. Earth and Planetary Science Letters, 2017, 477, 156-167.	1.8	16
84	Precambrian geology of the northern Nagssugtoqidian orogen, West Greenland: mapping in the Kangaatsiaq area. Geological Survey of Denmark and Greenland Bulletin, 0, 191, 13-23.	0.0	16
85	Rheology, microstructure and crystallographic preferred orientation of matrix containing a dispersed second phase: Insight from experimentally deformed ice. Earth and Planetary Science Letters, 2016, 449, 272-281.	1.8	15
86	Generation of amorphous carbon and crystallographic texture during low-temperature subseismic slip in calcite fault gouge. Geology, 2018, 46, 163-166.	2.0	15
87	Boom boom pow: Shock-facilitated aqueous alteration and evidence for two shock events in the Martian nakhlite meteorites. Science Advances, 2019, 5, eaaw5549.	4.7	15
88	The recognition of multiple magmatic events and pre-existing deformation zones in metamorphic rocks as illustrated by CL signatures and numerical modelling: examples from the Ballachulish contact aureole, Scotland. International Journal of Earth Sciences, 2012, 101, 1127-1148.	0.9	14
89	Simulation of surface dynamics during dissolution as a function of the surface orientation: Implications for non-constant dissolution rates. Earth and Planetary Science Letters, 2014, 408, 163-170.	1.8	14
90	Direct Observations of the Dissolution of Fluorite Surfaces with Different Orientations. Crystal Growth and Design, 2014, 14, 69-77.	1.4	14

#	Article	IF	CITATIONS
91	Pink color in Type I diamonds: Is deformation twinning the cause?. American Mineralogist, 2015, 100, 1518-1527.	0.9	14
92	Deformation behavior of migmatites: insights from microstructural analysis of a garnet–sillimanite–mullite–quartz–feldspar-bearing anatectic migmatite at Rampura–Agucha, Aravalli–Delhi Fold Belt, NW India. International Journal of Earth Sciences, 2018, 107, 2265-2292.	0.9	14
93	Sub-arc xenolith Fe-Li-Pb isotopes and textures tell tales of their journey through the mantle wedge and crust. Geology, 2018, 46, 947-950.	2.0	13
94	Tectonics of the Isua Supracrustal Belt 1: Pâ€Tâ€Xâ€d Constraints of a Polyâ€Metamorphic Terrane. Tectonics, 2021, 40, e2020TC006516.	1.3	13
95	Sintering of CaF2 pellets as nuclear fuel analog for surface stability experiments. Journal of Nuclear Materials, 2011, 419, 46-51.	1.3	12
96	Quantification of mineral behavior in four dimensions: Grain boundary and substructure dynamics in salt. Geochemistry, Geophysics, Geosystems, 2012, 13, .	1.0	12
97	Coupled extrusion of subâ€arc lithospheric mantle and lower crust during orogen collapse: a case study from Fiordland, New Zealand. Journal of Metamorphic Geology, 2016, 34, 501-524.	1.6	12
98	Time for anisotropy: The significance of mechanical anisotropy for the development of deformation structures. Journal of Structural Geology, 2019, 125, 41-47.	1.0	12
99	Inefficient high-temperature metamorphism in orthogneiss. American Mineralogist, 2019, 104, 17-30.	0.9	12
100	The influence of strain rate and presence of dispersed second phases on the deformation behaviour of polycrystalline D ₂ O ice. Journal of Glaciology, 2019, 65, 101-122.	1.1	12
101	Glimmerite: A product of melt-rock interaction within a crustal-scale high-strain zone. Gondwana Research, 2022, 105, 160-184.	3.0	12
102	Experimental modeling of viscous inclusions in a circular high-strain shear rig: Implications for the interpretation of shape fabrics and deformed enclaves. Journal of Geophysical Research, 2002, 107, ETG 11-1-ETG 11-15.	3.3	11
103	The application of GIS to unravel patterns of deformation in high grade terrains: a case study of indentor tectonics from west Greenland. Geological Society Special Publication, 2004, 224, 63-78.	0.8	11
104	Sillimanite deformation mechanisms within a Grt-Sil-Bt gneiss: effect of pre-deformation grain orientations and characteristics on mechanism, slip-system activation and rheology. Geological Society Special Publication, 2014, 394, 189-213.	0.8	11
105	Understanding the emplacement of Martian volcanic rocks using petrofabrics of the nakhlite meteorites. Earth and Planetary Science Letters, 2019, 520, 220-230.	1.8	11
106	Animations of dynamic recrystallization with the numerical modelling system Elle. Journal of the Virtual Explorer, 0, 04, .	0.0	11
107	Deformation microstructures reveal a complex mantle history for polycrystalline diamond. Geochemistry, Geophysics, Geosystems, 2012, 13, .	1.0	10
108	Surface morphology and structural types of natural impact apographitic diamonds. Journal of Superhard Materials, 2016, 38, 71-84.	0.5	10

#	Article	IF	CITATIONS
109	Maghemite soil nodules reveal the impact of fire on mineralogical and geochemical differentiation at the Earth's surface. Geochimica Et Cosmochimica Acta, 2017, 200, 25-41.	1.6	10
110	Full analysis of feldspar texture and crystal structure by combining X-ray and electron techniques. American Mineralogist, 2013, 98, 41-52.	0.9	9
111	In search of early life: Carbonate veins in Archean metamorphic rocks as potential hosts of biomarkers. Earth and Planetary Science Letters, 2016, 453, 44-55.	1.8	9
112	Microstructures reveal multistage melt present strain localisation in mid-ocean gabbros. Lithos, 2020, 366-367, 105572.	0.6	9
113	The evolution of ice fabrics: A continuum modelling approach validated against laboratory experiments. Earth and Planetary Science Letters, 2021, 556, 116718.	1.8	9
114	Tectonics of the Isua Supracrustal Belt 2: Microstructures Reveal Distributed Strain in the Absence of Major Fault Structures. Tectonics, 2021, 40, e2020TC006514.	1.3	9
115	The influence of triple junction kinetics on the evolution of polycrystalline materials during normal grain growth: New evidence from in-situ experiments using columnar Al foil. International Journal of Materials Research, 2005, 96, 1152-1157.	0.8	8
116	Time-lapse misorientation maps for the analysis of electron backscatter diffraction data from evolving microstructures. Scripta Materialia, 2011, 65, 600-603.	2.6	8
117	Strain localization in polycrystalline material with second phase particles: Numerical modeling with application to ice mixtures. Geochemistry, Geophysics, Geosystems, 2016, 17, 3608-3628.	1.0	8
118	Crystallography of refractory metal nuggets in carbonaceous chondrites: A transmission Kikuchi diffraction approach. Geochimica Et Cosmochimica Acta, 2017, 216, 42-60.	1.6	7
119	Fracturing and Porosity Channeling in Fluid Overpressure Zones in the Shallow Earth's Crust. Geofluids, 2020, 2020, 1-17.	0.3	7
120	Deformation Behavior and Inferred Seismic Properties of Tonalitic Migmatites at the Time of Preâ€melting, Partial Melting, and Postâ€Solidification. Geochemistry, Geophysics, Geosystems, 2021, 22, e2020GC009202.	1.0	7
121	Relative rates of fluid advection, elemental diffusion and replacement govern reaction front patterns. Earth and Planetary Science Letters, 2021, 565, 116950.	1.8	7
122	The Potential of Combined In-Situ Heating Experiments and Detailed EBSD Analysis in the Investigation of Grain Scale Processes such as Recrystallization and Phase Transformation. Materials Science Forum, 2004, 467-470, 1407-1412.	0.3	6
123	Substructure Dynamics in Crystalline Materials: New Insight from <i>In Situ</i> Experiments, Detailed EBSD Analysis of Experimental and Natural Samples and Numerical Modelling. Materials Science Forum, 2012, 715-716, 502-507.	0.3	6
124	Carbonado revisited: Insights from neutron diffraction, high resolution orientation mapping and numerical simulations. Lithos, 2016, 265, 244-256.	0.6	6
125	Palaeoproterozoic reworking of early Archaean lithospheric blocks: Rocks and zircon records from charnockitoids in Volgo-Uralia. Precambrian Research, 2021, 360, 106224.	1.2	6
126	Pressure, temperature and lithological dependence of seismic and magnetic susceptibility anisotropy in amphibolites and gneisses from the central Scandinavian Caledonides. Tectonophysics, 2021, 820, 229113.	0.9	6

#	Article	IF	CITATIONS
127	Seismic anisotropy of mid crustal orogenic nappes and their bounding structures: An example from the Middle Allochthon (Seve Nappe) of the Central Scandinavian Caledonides. Tectonophysics, 2021, 819, 229045.	0.9	5
128	Metamorphism in the New England Orogen, eastern Australia: a review. Australian Journal of Earth Sciences, 2020, 67, 453-478.	0.4	5
129	Grain Growth in Al: First Results from a Combined Study of Bulk and In-Situ Experiments Using a Columnar Structured Al Foil. Materials Science Forum, 2004, 467-470, 935-940.	0.3	4
130	The Weighted Burgers Vector: A Quantity for Constraining Dislocation Densities and Types Using Electron Backscatter Diffraction on 2D Sections through Crystalline Materials. Materials Science Forum, 0, 715-716, 732-736.	0.3	4
131	The Application of <i>In Situ</i> 3D X-Ray Diffraction in Annealing Experiments: First Interpretation of Substructure Development in Deformed NaCl. Materials Science Forum, 2012, 715-716, 461-466.	0.3	4
132	Determining relative bulk viscosity of kilometre-scale crustal units using field observations and numerical modelling. Tectonophysics, 2017, 721, 275-291.	0.9	4
133	Characterization of Ultra-fine Grained and Nanocrystalline Materials Using Transmission Kikuchi Diffraction. Journal of Visualized Experiments, 2017, , .	0.2	4
134	Metamorphic Differentiation via Enhanced Dissolution along High Permeability Zones. Journal of Petrology, 2021, 61, .	1.1	4
135	Local variations of metamorphic record from compositionally heterogeneous rocks (Cima di) Tj ETQq1 1 0.78431 106126.	4 rgBT /O 0.6	verlock 10 Tf 4
136	Experimental deformation of deuterated ice in 3D and 2D: identification of grain-scale processes. Proceedings of the Royal Society of Victoria, 2015, 127, 99.	0.3	4
137	Oxide enrichment by syntectonic melt-rock interaction. Lithos, 2022, 414-415, 106617.	0.6	4
138	Annealing in a Natural Laboratory: an EBSD and Cl Study of Calcite and Quartz Growth from Volumes of Rock Heated by a Nearby Melt Intrusion. Materials Science Forum, 2007, 550, 333-338.	0.3	3
139	A deep rock laboratory in the Dellen impact crater. Gff, 2010, 132, 45-54.	0.4	3
140	Ductile Deformation Without Localization: Insights From Numerical Modeling. Geochemistry, Geophysics, Geosystems, 2019, 20, 5710-5726.	1.0	3
141	New apparatus for controlled general flow modeling of analog materials. , 2001, , .		2
142	Quantitative Analysis of EBSD Data in Rocks and other Crystalline Materials: Investigation of Strain Induced Recrystallisation and Growth of New Phases. Materials Science Forum, 2012, 715-716, 62-71.	0.3	2
143	Two belts of HTLP sub-regional metamorphism in the New England Orogen, eastern Australia: occurrence and characteristics exemplified by the Wongwibinda Metamorphic Complex. Australian Journal of Earth Sciences, 2020, 67, 479-507.	0.4	2
144	Constraints on the Emplacement of Martian Nakhlite Igneous Rocks and Their Source Volcano From Advanced Microâ€Petrofabric Analysis. Journal of Geophysical Research E: Planets, 2022, 127, .	1.5	2

#	Article	IF	CITATIONS
145	Role of inherited compositional and structural heterogeneity in shear zone development at mid-low levels of the continental crust (the Anzola shear zone; Ivrea-Verbano Zone, Southern Alps). Lithos, 2022, 422-423, 106745.	0.6	2
146	Non-Destructive Residual Stress Investigations of Natural Polycrystalline Diamonds. Advanced Materials Research, 0, 996, 969-974.	0.3	1
147	Legacy base metal slags can generate toxic leachates. Powder Diffraction, 2017, 32, S70-S77.	0.4	1
148	Can the Magmatic Conditions of the Martian Nakhlites be Discerned via Investigation of Clinopyroxene and Olivine Intracrystalline Misorientations?. Journal of Geophysical Research E: Planets, 2022, 127, .	1.5	1
149	Reply to Comment by Nutman etÂal. on "Tectonics of the Isua Supracrustal Belt I and II― Tectonics, 0, , .	1.3	1
150	Exploring Innovative and Challenging Applications of EBSD in the Geological and Biological Sciences. Microscopy and Microanalysis, 2011, 17, 412-413.	0.2	0
151	Investigation of fabrics in quartz and ice: comparison and applications of different analytical methods. Geotectonic Research, 2015, 97, 100-102.	0.1	0
152	Quantitative microstructural analysis of geological materials by atom probe: understanding the mechano-chemical behaviour of zircon. Microscopy and Microanalysis, 2015, 21, 1317-1318.	0.2	0
153	The Use of High Speed, High Resolution EBSD to Unlock Hidden Secrets of the Allende Meteorite. Microscopy and Microanalysis, 2018, 24, 2082-2083.	0.2	0
154	The Importance of Physiochemical Processes in Decarbonisation Technology Applications Utilizing the Subsurface: A Review. Earth Science, Systems and Society, 0, 2, .	0.0	0